Tuning avalanche criticality: Acoustic emission during the martensitic transformation of a compressed Ni-Mn-Ga single crystal

R. Niemann,[1,2,*] J. Baró,[3] O. Heczko,[4] L. Schultz,[1,2] S. Fähler,[1,2] E. Vives,[3] L. Mañosa,[3] and A. Planes[3]

[1]*IFW Dresden, P.O. Box 270116, 01171 Dresden, Germany*

[2]*Department of Physics, Institute for Solid State Physics, Dresden University of Technology, 01062 Dresden, Germany*

[3]*Departament d'Estructura i Constituents de la Matèria, Facultat de Física, Universitat de Barcelona, Diagonal 647, 08028 Barcelona, Catalonia, Spain*

[4]*Institute of Physics, Academy of Science of the Czech Republic, Na Slovance 2, 182 02 Prague, Czech Republic*

(Received 3 September 2012; published 3 December 2012)

The propagation of a phase front during a thermally induced martensitic transition is discontinuous due to pinning at various defects, an effect which results in acoustic emission. Here we analyze the consequences of an applied compressive stress exemplarily on a $Ni_{50.4}Mn_{27.9}Ga_{21.7}$ single crystal. Our experiments show that the distribution of the energies of the acoustic emission events follows a power law for more than three decades. This indicates that the transition exhibits avalanche criticality. The exponent characterizing the distribution of energies depends on the applied stress, and decreases from 1.9 ± 0.1 at zero stress to 1.5 ± 0.2 at stress above 3 MPa. This decrease could be attributed to the reduced multiplicity of variants possible under uniaxial compression.

DOI: 10.1103/PhysRevB.86.214101 PACS number(s): 81.30.Kf, 64.60.av, 43.90.+v

I. INTRODUCTION

A martensitic transformation is a diffusionless structural phase transition, which transforms a crystal structure with high symmetry to one with lower symmetry. In general, martensitic transformations display jerky dynamics.[1] This means when these systems are externally driven, the transition proceeds discontinuously as a sequence of jerks and therefore belongs to the wide variety of physical systems that exhibit crackling noise.[2] In martensitic systems, the jerks (also called avalanches) are associated with local discontinuities of the order parameter (strain) and reflect the fact that the system relaxes from one metastable state to another metastable state within a complex energy landscape which characterizes the region with two phases coexisting. The metastable minima are commonly separated by high energy barriers and consequently the dynamics are not controlled by thermal activation effects but instead exhibit an athermal character.[3] During these fast local relaxation events, the system dissipates the excess of elastic energy accumulated during the transition process.[4] This energy is partly dissipated in the form of high-frequency acoustic waves which originate from displacement discontinuities across the propagating interfaces and occur in the frequency range between kHz and MHz. This is the well known acoustic emission (AE) characteristic of martensitic transitions.[5] Monitoring the AE is a convenient experimental technique to study avalanches in martensitic transitions. The statistical distribution of the energy and amplitude of the AE events provides relevant information concerning the dynamics of this class of structural transitions. In particular, avalanche criticality is detected from a power-law behavior of these distributions. Actually, the presence of a power-law dependency is a signature that the system evolves through the energy landscape in the absence of characteristic time and size scales of the avalanches.

The power-law exponent is the key indicator characterizing avalanche criticality. In particular, the exponent depends on the symmetry and dimension of the underlying martensitic transition. Experiments reveal that the power-law exponent is lower when the product martensite exhibits a high crystal symmetry, which allows only for a low number of different variant orientations.[6] In other words, the multiplicity of all product variants is important. Furthermore, it is important how many dimensions the propagating interface comprises.[7] In simulations also the dimensionality of the system can be varied and a decrease of the exponent for reduced dimensions has been reported.[8,9] As in low dimensions only a low number of variant orientations is possible, this is equivalent to a reduction of multiplicity.

Here we will experimentally probe the influence of a compressive stress on the critical exponent. The idea for the experiments is that the compressive stress reduces the dimensionality wherein the martensitic variants can be oriented. Without stress, alignment of variants in a three-dimensional space is possible. Compressive stress constrains the alignment to a two-dimensional plane perpendicular to stress direction. For this, we apply different external mechanical fields during a thermally induced martensitic transition, which inhibits certain variant orientations. As a model system we selected a single crystal of the Ni-Mn-Ga magnetic shape memory alloy. As their functionalization for magnetically controlled actuators requires highly mobile twin boundaries, samples are available in which a low stress in the order of 1 MPa is sufficient to select between different variant orientations.[10,11] In this multiferroic material the influences of both stress and magnetic fields[12] on structure and microstructure are well known.[13,14] In particular the influence of an applied magnetic field on AE in premartensitic and martensitic transformations has been reported recently.[15,16]

The present paper is organized as follows. First, we describe the experimental setup, procedure, and data acquisition. Then, we present the resulting acoustic emission as a function of temperature for different applied stress fields. Finally, we discuss our findings with respect to constraints induced by stress fields, and generalize them by the comparison with recent experiments under magnetic fields. We suggest that the

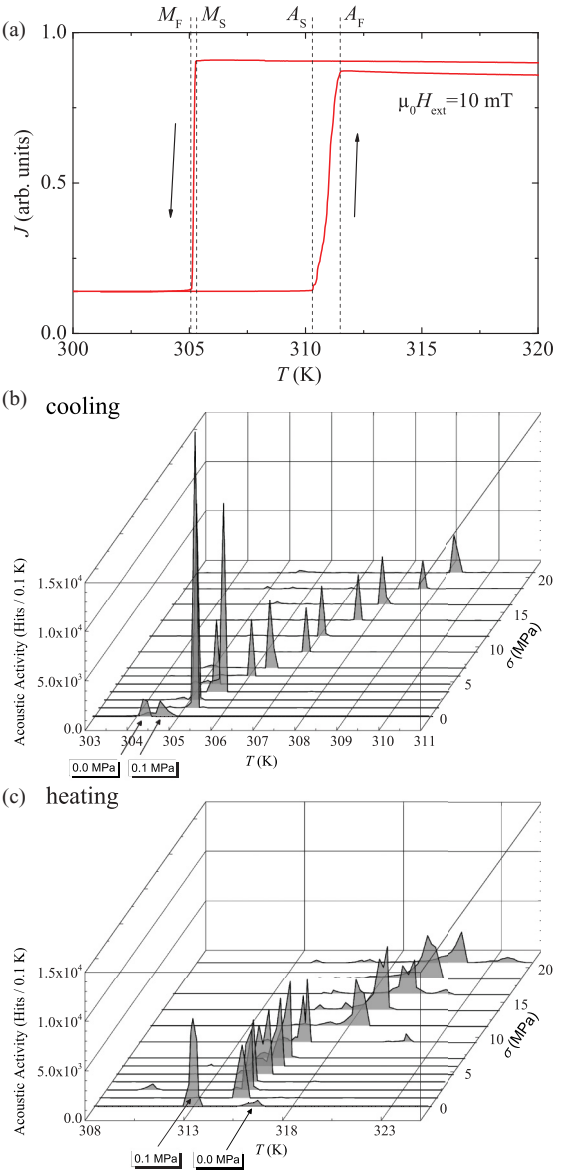

FIG. 1. (Color online) (a) Magnetic polarization in 10 mT external magnetic field as a function of temperature. Arrows indicate the heating and cooling branches. The transformation temperatures are marked. (b) Acoustic activity as a function of temperature for different applied stresses during cooling (austenite to martensite transformation) and (c) heating (martensite to austenite transformation).

decrease of critical exponents under universal fields originates from the reduced multiplicity in the martensitic microstructure and not from the influence of external fields on the martensitic crystal structure.

II. EXPERIMENTAL PROCEDURE, DATA ACQUISITION AND ANALYSIS

We used a $Ni_{50.4}Mn_{27.9}Ga_{21.7}$ single crystal ($e/a = 7.644$) in the form of a $4.8 \times 5.8 \times 9.5$ mm^3 cuboid with faces parallel to the {100} crystallographic planes of the parent cubic $L2_1$ austenite phase. The structure at room temperature is 10M martensite, which is typical for this composition.[17] Magnetic polarization was measured in a Quantum Design Physical Property Measurement System with vibrating sample magnetometer option. From a temperature-dependent measurement of the magnetic polarization at 2 K/min in an external magnetic field of 0.01 T [Fig. 1(a)] that reveals a sharp change in polarization connected with a hysteresis in the vicinity of 307 K, we determined the martensitic transformation temperatures $M_S = 305.3$ K, $M_F = 305.1$ K, $A_S = 310.3$ K, and $A_F = 311.6$ K. The Curie temperature of the sample is $T_C = 377.6$ K.

For the acoustic emission experiment, the sample was placed between two aluminum compression plates and different weights were attached to the top plate. This enabled us to apply uniaxial compressive stress along the [100] crystallographic direction of austenite parallel to the 5.8 mm long edge of the sample. The compression device was situated inside a temperature chamber. The temperature was measured by a Pt100 resistance sensor coupled to the acoustic emission measurement system.

Initially, the sample was heated to 341 K to bring it into the austenitic state. Then, a compressive stress (load) was applied. At constant load, the sample was cooled to 298 K and then heated again to 341 K while the acoustic activity was recorded. Being in the austenitic state again, the load was increased. This was performed using several loads from 0 to 20.7 MPa.

The acoustic emission during heating and cooling under constant load was detected with two piezoelectric PAC Micro 80 transducers mounted inside the compression plates near the top and bottom of the sample. The signals were preamplified (60 dB), acquired by a PCI-2 card from Europhysical Acoustics (Mistras Group) at a rate of 10 Msamples/s and passed through an analog filter between 20 kHz and 2 MHz. A signal was stored if its amplitude was above a threshold level of 31 dB for the transducer in the top plate and of 30 dB for the transducer in the bottom plate. The acoustic activity was recorded separately for each transformation experiment in the form of a list of single events (hits) where the time, temperature, and absolute energy of each event were also included.

First, this list was separated into time intervals of 10 s and the number of hits in each interval was counted. Additionally, the average temperature and temperature rate for each interval were calculated. Some intervals in the vicinity of the martensitic transformation temperature contained several 10^4 hits, but most only several 10 hits. This was attributed to background noise and we subtracted the average noise level. Afterwards, the number of events in each time interval was divided by the average temperature rate to cancel out variations in the rates that could not be avoided for technical reasons. Finally, the resulting numbers of hits per rate per time interval were assigned to their average temperature. Then these values were sampled in steps of 0.1 K. The result is the acoustic activity as a function of temperature.

III. RESULTS

The resulting acoustic activity as a function of temperature for all loads is shown separately for cooling [Fig. 1(b)] and heating [Fig. 1(c)]. The temperature interval shown is confined from 303 to 311 K for cooling and from 310 to 325 K

for heating. No acoustic activity above the noise level was recorded outside these intervals. Since the peaks of acoustic activity at zero stress coincide with the maximum change in magnetization with temperature, the acoustic activity inside the intervals can be attributed to the acoustic emission of a martensitic transformation.

For all applied loads, the acoustic activity in the transformation interval is confined within a peak of 1 to 2 K width for heating and 0.2 to 0.4 K width for cooling. The maximum activity is in the order of 10^4 hits/(0.1 K) for heating and 3×10^4 hits/(0.1K) for cooling. Since the transformation to austenite occurs in a broader temperature interval, the integrated acoustic activity was always larger for heating (order of 10^9 hits) than for cooling (10^8 hits). The broader temperature interval of the transformation during heating was also observed in the temperature-dependent measurements of the magnetic polarization [Fig. 1(a)].

The temperatures of the forward (austenite to martensite) and reverse (martensite to austenite) transformations were defined using the mean of a Gaussian fit to the peaks of acoustic emission. The transformation temperatures determined by acoustic emission measurement deviate by a few Kelvin from the results of the temperature-dependent magnetization measurement especially during heating because of the different temperature measurement setups used. The dependence of the transformation temperatures on the applied stress is depicted in Fig. 2. They show an almost linear increase of 0.36 K/MPa on heating and 0.22 K/MPa on cooling. There is a substantial scattering for low loads. We attribute this to the rough twinned surface of the crystal in the martensitic state which weakens the thermal contact between the sample and the top compression plate, where the temperature was measured. The dependence of the transformation temperature on the external stress was reported to be linear with a slope of 0.11 K/MPa in $Ni_{52.0}Mn_{24.4}Ga_{23.6}$ ($e/a = 7.62$).[18] In our experiments, the slope was significantly higher. This is a consequence of the different composition: The slope is strongly dependent on the different temperature dependence of the free energy of austenite and martensite under stress[19,20] and thus on composition[21] and chemical order.[22]

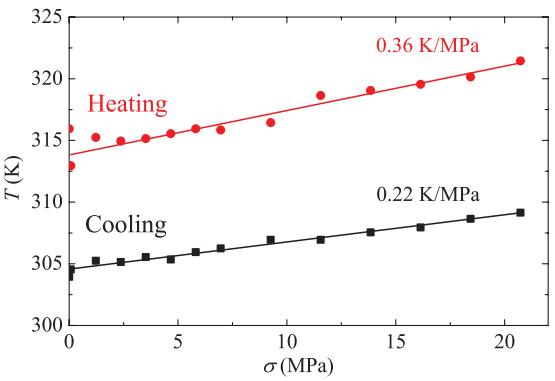

FIG. 2. (Color online) Transformation temperatures defined by the peak of acoustic activity as a function of the applied stress σ during cooling (forward transformation) and heating (reverse transformation). To quantify the change with mechanical stress, a linear regression was applied.

For avalanche criticality it is expected that the distribution of the energy E of the AE events emitted during a martensitic transformation follows a power law, described by the probability density function

$$p(E)\mathrm{d}E = C_\varepsilon E^{-\varepsilon}\mathrm{d}E.$$

Here $p(E)$ is the probability density, C_ε is a normalization factor, and ε is called the critical exponent. This exponent exhibits a certain degree of universality, depending only on the crystal symmetry of the martensite and the driving field.[6] The distribution of acoustic emission hits during heating in the transformation interval is easily accessible in the form of a histogram. It shows the number of hits per energy interval. For clarity, we display only a few loads (Fig. 3). We chose a double-logarithmic plot and logarithmic energy intervals (logarithmic binning with 7 bins/decade). In this plot, a power-law distribution would appear as a straight line with the slope $1 - \varepsilon$. Within the energy range from 1 to 10^3 aJ this linear dependence is followed well. The measured distribution deviates from power law for very low energies because it is superimposed by noise with Gaussian distribution and for very high energies because of the finite size of the sample and saturation limits of the measurement device.

There are several ways to extract the exponent ε.[23] The easiest way is to determine the slope in a double-logarithmic plot of the energy histogram by linear regression, but least-square fitting methods mostly lack accuracy because they depend on the chosen binning intervals. The most reliable method to analyze power-law distributed data, which is totally independent of data binning, is the maximum likelihood method.[24] This method provides a robust value for the exponent ε and its error bar, and at the same time gives an estimation for the lower energy boundary (E_{low}) of the validity of this exponent. If the data follow a power law, a plateau of constant ε will extend over several decades of E_{low}. Recently, also maximum likelihood (ML) maps were proposed,[23,25] where additionally an upper energy boundary (E_{high}) is introduced as a second variable. This upper limit of energy becomes necessary because the measurement device

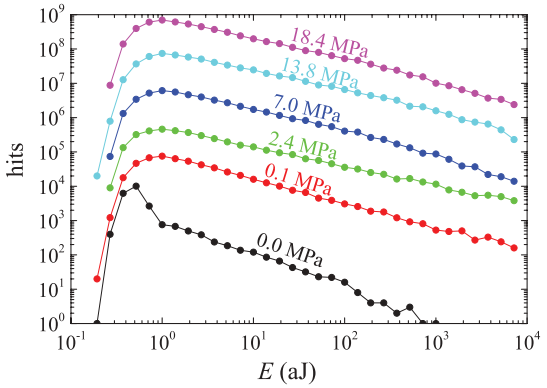

FIG. 3. (Color online) Energy histograms of number of hits vs energy for external compressive stresses between 0 and 20.7 MPa in the transformation interval during heating (reverse transformation). The energy intervals are also plotted logarithmically. The histograms are multiplied by increasing powers of ten for increasing loads to obtain an offset of the curves for clarity.

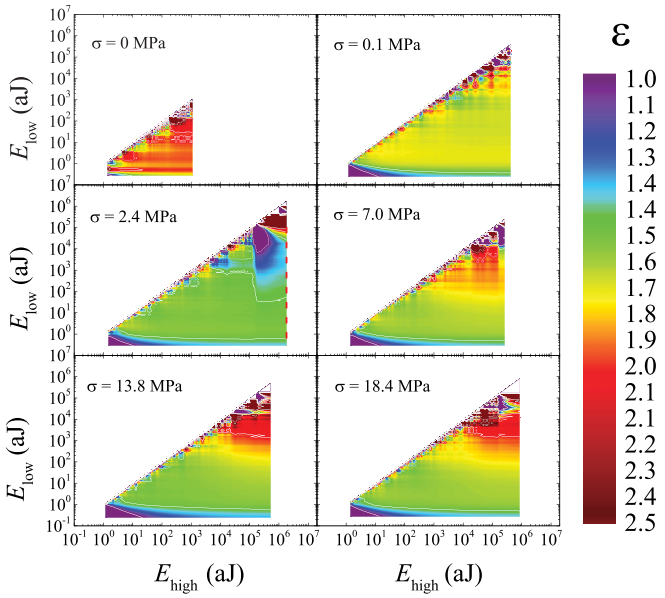

FIG. 4. (Color online) Maximum likelihood maps for a selection of transformations from martensite to austenite under load. The energy exponent that describes the energy distribution within the boundaries E_{low} and E_{high} is color coded. White lines mark a change in the first digit of the exponent in steps of 0.1.

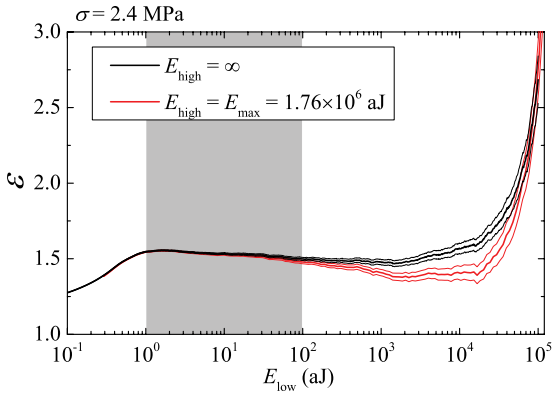

FIG. 5. (Color online) Exponent ε as a function of E_{low} using the maximum likelihood method (thick lines) including error intervals (thin lines) exemplarily for a medium load of 2.4 MPa. The red line coincides with a profile of the likelihood map for maximum $E_{high} = E_{max}$ (marked with a dashed red line in Fig. 4). The black line is independently calculated for $E_{high} = \infty$.

may become saturated by too strong or too long signals. These signals will be either dropped completely or truncated, which distorts the histogram. The energy released during the strongest event recorded is called E_{max}. Generally in ML maps the exponent is color coded as a function of E_{low} and E_{high}. If the data follow a power law, a plateau of constant exponent will appear inside the map marked by homogeneous color extending over several square decades of E_{low} and E_{high}. We show the ML maps in Fig. 4 for the identical selection of experiments that was presented in Fig. 3. As expected, all maps comprise an area of constant exponent, hence our experiments have a power-law distribution within the energy limits E_{low} and E_{high}. Notably the maps have different sizes, which means that the maximum energy recorded in each experiment is different. Most prominent is the experiment at 0 MPa, which shows maximum energies of only 10^3 aJ while all others comprise maximum energies of more than 10^5 aJ. The reason is that, in the stress-free experiment, the top compression plate was removed. We expect that the acoustic coupling to the transducer in the bottom plate was lowered and no high-energy events could be recorded. The variation in maximum energy between all other experiments with applied load is much smaller. A plateau is always encountered in a rectangle between $E_{low} = 1$ aJ, $E_{high} = 10^3$ aJ and $E_{low} = 10$ aJ, $E_{high} = E_{max}$.

To analyze the exponent in quantitative detail, we plotted a profile through the map at $E_{high} = E_{max}$, which gives the exponent as a function of E_{low}. Additionally, the exponent was analyzed as a function of E_{low} with the standard maximum likelihood method, which is equivalent to consider an infinite E_{high}. Both curves are shown exemplarily for one experiment at $\sigma = 2.4$ MPa in Fig. 5. The deviation between curves in the interval from $E_{low} = 1$ aJ to $E_{low} = 100$ aJ is within the error bars of both methods. A detailed discussion about the fundamental difference of both methods can be found in Ref. 23. Finally, we determined the exponent for all experiments during heating by calculating an error-weighted mean from $E_{low} = 1$ aJ to $E_{low} = 100$ aJ at $E_{high} = E_{max}$. This interval is marked in grey in Fig. 5. The error is defined as half of the difference between $\bar{\varepsilon}$ and $\varepsilon(E_{low} = 1$ aJ).

The determined ε of all transformation experiments is plotted as function of the applied load in Fig. 6. For zero load, the exponent is maximum around 1.9 but with a relatively big error of 0.1 because of the small number of events. For the smallest applied load of 0.1 MPa, which is just due to the weight of the top compression plate, the exponent is 1.7 with a smaller error. For loads above 2.5 MPa there is a scattering between 1.65 and 1.4, but all values remain substantially below the stress free state. A linear crossover at 2.5 MPa is plotted as guide to the eye.

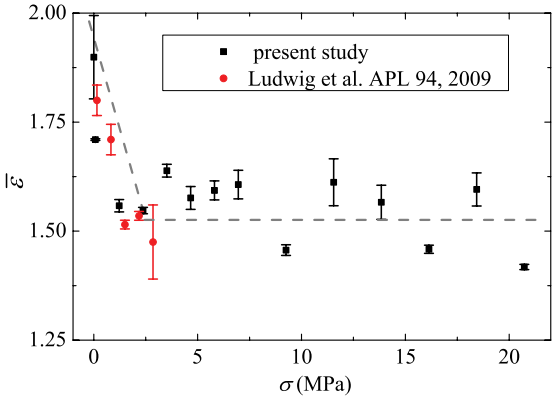

FIG. 6. (Color online) Exponent determined by averaging the maximum likelihood functions in the marked interval of Fig. 5 for the transformation from martensite to austenite as a function of applied compressive stress. Additionally, results by Ludwig *et al.* (Ref. 15) are plotted, where a magnetic field is recalculated according to magnetostress acting upon the variants.

IV. DISCUSSION

In the present work we have reported results of the AE during the thermally induced martensitic transition in a $Ni_{50.4}Mn_{27.9}Ga_{21.7}$ magnetic shape memory single crystal. We have studied the effect of an applied compressive stress on the statistical distribution of the energies of the AE events. The detection of AE has confirmed that, regardless of the applied compressive stress, transition dynamics in Ni-Mn-Ga shape memory alloy displays jerky character. In all studied cases, the energy of the AE events exhibits a power-law behavior within more than four decades. This enables us to conclude that, within a very good approximation, avalanche criticality occurs independently of the applied stress.

The multiferroic properties of magnetic shape memory alloys allows us to probe our concept by using different types of fields. Recently Ludwig *et al.*[15] applied constant magnetic fields while measuring the acoustic activity of a 10M $Ni_{52}Mn_{23}Ga_{25}$ single crystal during thermally induced martensitic transformation. They observed that the acoustic emission amplitude A also follows a power law. A significant decrease of the corresponding exponent α from 2.6 to 2.1 for increasing magnetic field up to 0.8 T was observed.[15] This corresponds to a decrease in ε from $\approx$1.8 to $\approx$1.5, which is a very good agreement with the present experiments under compressive stress.[26] This implies that both types of fields act in the same way: they reduce the multiplicity. While a stress field constrains the alignment of the crystallographic axes, the magnetic field aligns the easy magnetic axis. Since the short crystallographic c axis of 10M is at the same time the magnetic easy axis, both a magnetic field and a compressive stress will favor variants with the c axis in the direction of the field and compression direction, respectively.[27]

An absolute comparison of both fields is possible when using the concept of the equivalent stress caused by a magnetic field, which is called magnetostress. The magnetostress as a function of magnetic field for 10M single crystals can be calculated[28] and was reported, e.g., by Heczko *et al.*[29] and Müllner *et al.*[30] and collected by Karaca.[31] Up to the anisotropy field of 0.8 T,[32] a linear dependence between both fields can be used, so the magnetostress can be calculated by $\sigma(H) = \beta \times H$ where $\beta = 3.4$ MPa/T with an error of 0.3 MPa/T. This is only an approximation since the slope β depends on the particular shape of the sample and the corresponding demagnetization factor, which determines the internal magnetic field. Additionally, in the work by Ludwig *et al.*, a small compressive stress $\sigma_0 = 0.15$ MPa was applied additionally perpendicular to the magnetic field to fix the sample in place.[15] This can lead to an additional influence on the variant selection. We took this into account by using an effective magnetostress on the variants: $\sigma(H)_{\text{eff}} = \beta \times H + \sigma_0$. Even if this estimation is relatively rough, this stress to align the sample is within the error of the estimation of the magnetostress and small compared to the maximum magnetostress, so it has no big influence on the obtained results. But it is important to note that the case of zero applied magnetic field is not fully stress free.

The exponent ε by Ludwig *et al.* as a function of the magnetostress is plotted additionally to our results in Fig. 6. The maximum effective magnetostress of about 2.7 MPa is one order of magnitude smaller than our maximum applied compressive stress since the maximum magnetostress reachable is limited by magnetocrystalline anisotropy. The values for ε from both sets of measurements coincide very well. This shows that stress and magnetic field have a very similar influence on the statistics of the acoustic emission generated by the martensitic transformation.

As a key finding, we observe that the exponent characterizing the power laws decreases from a value of 1.9 ± 0.1 to 1.5 ± 0.2 when the stress increases from zero to 2.5 MPa and remains constant for larger applied stresses. We will discuss this behavior with respect to the multiplicity of the different variant orientations possible. The martensite studied here is 10M, which has a monoclinic crystal symmetry,[33] and allows for a multiplicity of 12.[34] The observed critical exponent for the stress-free state agrees well with the value of 2.0 ± 0.2 for other monoclinic martensites.[35] Though the very moderate stress level used here is not expected to affect the crystal symmetry, we observe a decrease of the exponent to 1.5 ± 0.2 under stress. Usually, such a lower exponent is found for martensites with a lower variant multiplicity.[6] FePd for example, which transforms into a tetragonal martensite with a multiplicity of only 3, exhibits an exponent of only 1.6 ± 0.1.[36]

We suggest considering the influence of a stress field as a constraint reducing the multiplicity. An applied uniaxial compressive stress favors the formation of variants with their short crystallographic axes in the stress direction. For the monoclinic 10M unit cell this leaves only four possibilities to align the unit cell. A sufficient compressive stress can therefore reduce the variant multiplicity from 12 to 4 and accordingly reduce the number of possible transformation paths and lower the critical exponent.

In our experiments we observe that the crossover is finished already at a low stress level of 2.5 MPa. This stress level is close to the stress of 1 MPa required to move twin boundaries in a sample cut from the same crystal.[27] Hence both the reduced critical exponent and the crossover stress field can be explained by the reduced multiplicity by uniaxial compression.

Our analysis benefits significantly from this low twinning stress as it allows excluding the other effects of stress on these multiferroic systems. The stress itself can shift the martensitic transformation temperature. Due to the low twinning stress, however, a shift of only 5.5 K is observed at the maximum stress applied, which is negligible compared to the martensitic transformation temperature of 305 K. Furthermore, stress can induce an intermartensitic transition from a modulated to a simple tetragonal martensite. This process can also be interpreted as coarsening of adaptive martensite, but occurs at significantly higher stress levels than used here,[37] thus the effect of an intermartensitic transformation can be excluded.

For a martensitic transformation, the sign of the stress is important. Often, substantial asymmetries are observed between tensile and compressive stress.[38] The study of the AE during the tensile stress induced martensitic transformation (at constant temperature) in a Cu-Zn-Al single crystal was reported.[39] The exponent of the distribution of avalanche energies was found to coincide, within the errors, with the exponent

found during the temperature-induced transformation (at zero applied stress) to a polyvariant monoclinic martensite. To understand the fundamental difference between compressive and tensile stress, it is sufficent to consider a tetragonal approximation. Both, the monoclinic 18R phase in Cu-based Heusler alloys, as well as 10M in Ni-based Heusler alloys, can be approximated as pseudotetragonal structures with $c < a$.[34] A tensile stress along a main crystallographic axis of the parent phase will favor both long axes (or disfavor the short axis) in comparison to a compressive stress that will favor the single short axis (or disfavor the long axis). So a tensile experiment reduces the variant multiplicity for monoclinic variants from 12 to only 8 while a compressive stress leaves only 4 variants to select from.

To summarize, our result enables to conclude that variant multiplicity is the main factor controlling the transformation dynamics in magnetic shape-memory alloys in a nonlinear way. To understand the microscopic mechanism in more detail, we suggest examining the nucleation, growth, and morphology of the phase boundaries in more detail.

ACKNOWLEDGMENTS

This work has been funded by DFG through SPP 1239, by CICyT (Spain) through Project No. MAT2010-15114, and by the Czech Scientific Foundation through Grant No. P107/11/0391. We thank A. Backen and A. Diestel for helpful discussions.

*Corresponding author: r.niemann@ifw-dresden.de

[1] E. Vives, J. Ortín, L. Mañosa, I. Ràfols, R. Pérez-Magrané, and A. Planes, Phys. Rev. Lett. **72**, 1694 (1994).
[2] J. Sethna, K. A. Dahmen, and C. R. Myers, Nature (London) **410**, 242 (2001).
[3] F. J. Pérez-Reche, E. Vives, L. Mañosa, and A. Planes, Phys. Rev. Lett. **87**, 195701 (2001).
[4] M. C. Gallardo, J. Manchado, F. J. Romero, J. del Cerro, E. K. H. Salje, A. Planes, E. Vives, R. Romero, and M. Stipcich, Phys. Rev. B **81**, 174102 (2010).
[5] Z. Yu and P. C. Clapp, J. Appl. Phys. **62**, 2212 (1987).
[6] A. Planes, L. Mañosa, and E. Vives, J. Alloys Compd. (2011), doi: 10.1016/j.jallcom.2011.10.082.
[7] E. K. H. Salje, Solid State Phen. **172**, 3 (2011).
[8] J. Ortín, I. Ràfols, L. Carrillo, J. Goicoechea, E. Vives, L. Mañosa, and A. Planes, J. Phys. IV **5**, C8 (1995).
[9] R. Ahluwalia and G. Ananthakrishna, Phys. Rev. Lett. **86**, 4076 (2001).
[10] A. Sozinov, A. A. Likhachev, N. Lanska, and K. Ullakko, Appl. Phys. Lett. **80**, 1746 (2002).
[11] L. Straka, O. Heczko, H. Seiner, N. Lanska, J. Drahokoupil, A. Soroka, S. Fähler, H. Hänninen, and A. Sozinov, Acta Mater. **59**, 7450 (2011).
[12] L. Straka, O. Heczko, V. Novak, and N. Lanska, J. Phys. IV **112**, 911 (2003).
[13] M. Chmielus, V. A. Chernenko, W. B. Knowlton, G. Kostorz, and P. Müllner, Eur. Phys. J. Spec. Top. **158**, 79 (2008).
[14] N. Okamoto, T. Fukuda, T. Kakeshita, T. Takeuchi, and K. Kishio, Sci. Technol. Adv. Mater. **5**, 29 (2004).
[15] B. Ludwig, C. Strothkaemper, U. Klemradt, X. Moya, L. Mañosa, E. Vives, and A. Planes, Appl. Phys. Lett. **94**, 121901 (2009).
[16] B. Ludwig, C. Strothkaemper, U. Klemradt, X. Moya, L. Mañosa, E. Vives, and A. Planes, Phys. Rev. B **80**, 144102 (2009).
[17] N. Lanska, O. Soderberg, A. Sozinov, Y. Ge, K. Ullakko, and V. K. Lindroos, J. Appl. Phys. **95**, 8074 (2004).
[18] V. A. Chernenko, J. Pons, E. Cesari, and K. Ishikawa, Acta Mater. **53**, 5071 (2005).
[19] K. Otsuka and C. M. Wayman, *Shape Memory Materials* (Cambridge University Press, Cambridge, UK, 1998).
[20] H. E. Karaca, B. Basaran, I. Karaman, and Y. I. Chumlyakov, Smart Mater. Struct. **21**, 045011 (2012).
[21] X. Jin, M. Marioni, D. Bono, S. M. Allen, R. C. O'Handley, and T. Y. Hsu, J. Appl. Phys. **91**, 8222 (2002).
[22] V. Sánchez-Alarcos, V. Recarte, J. Pérez-Landazábal, and G. J. Cuello, Acta Mater. **55**, 3883 (2007).
[23] J. Baro and E. Vives, Phys. Rev. E **85**, 066121 (2012).
[24] A. Clauset, C. Rohilla-Shalizi, and M. E. J. Neuman, SIAM Rev. **51**, 661 (2009).
[25] O. Peters, A. Deluca, A. Corral, J. Neelin, and C. Holloway, J. Stat. Mech. (2010) P11030.
[26] The acoustic emission amplitude A is connected to the energy E by the scaling relation $E \sim A^2$. The critical exponent α of A can be converted to the critical exponent ε through $\varepsilon = (\alpha + 1)/2$; see Refs. 15 and 36.
[27] O. Heczko and L. Straka, J. Appl. Phys. **94**, 7193 (2003).
[28] L. Straka and O. Heczko, IEEE Trans. Magn. **39**, 3402 (2003).
[29] O. Heczko and L. Straka, Mater. Sci. Eng. A **378**, 394 (2004).
[30] P. Müllner, V. A. Chernenko, and G. Kostorz, J. Magn. Magn. Mater. **267**, 325 (2003).
[31] H. E. Karaca, I. Karaman, and B. Basaran, Acta Mater. **54**, 233 (2006).
[32] L. Straka and O. Heczko, J. Appl. Phys. **93**, 8636 (2003).
[33] L. Righi, F. Albertini, L. Pareti, A. Paoluzi, and G. Calestani, Acta. Mater. **55**, 5237 (2007).
[34] K. Bhachattarya, *Microstructure of Martensite* (Oxford University Press, Oxford, 2007).
[35] L. Carrillo, L. Mañosa, J. Ortín, A. Planes, and E. Vives, Phys. Rev. Lett. **81**, 1889 (1998).
[36] E. Bonnot, L. Manosa, A. Planes, D. Soto-Parra, E. Vives, B. Ludwig, C. Strothkaemper, T. Fukuda, and T. Kakeshita, Phys. Rev. B **78**, 184103 (2008).
[37] R. Niemann, U. K. Rößler, M. E. Gruner, O. Heczko, L. Schultz, and S. Fähler, Adv. Eng. Mater. **14**, 562 (2012).
[38] E. Panchenko, Y. Chumlyakov, H. J. Maier, E. Timofeeva, and I. Karaman, Intermetallics **18**, 2458 (2010).
[39] E. Vives, D. Soto-Parra, L. Mañosa, R. Romero, and A. Planes, Phys. Rev. B **80**, 180101(R) (2009).